JOURNAL OF COLLOID AND INTERFACE SCIENCE **179,** 66–75 (1996)
ARTICLE NO. 0189

Role of Surface Tension Gradients in Correcting Coating Defects in Corners

D. E. WEIDNER,* L. W. SCHWARTZ,*,†,[1] AND R. R. ELEY‡

*Departments of *Mechanical Engineering and †Mathematical Sciences, University of Delaware, Newark, Delaware 19716; and ‡Glidden Company, Member ICI Paints, 16651 Sprague Road, Strongsville, Ohio 44136*

Received April 3, 1995; accepted October 25, 1995

Following the application of a liquid coating to a curved substrate, surface tension forces will act to redistribute the coating layer. The coating will thin at outside corners and thicken at inside corners as the free surface contracts to minimize the surface energy. If the coating is a multicomponent liquid with a volatile component, the dynamics of the thinning process may be quite complex. Compositional changes in the bulk liquid during drying and convection of surfactant may cause surface tension gradient or Marangoni effects. In addition there may be viscosity variations due to concentration changes and the liquid may exhibit shear-thinning rheology. A numerical model has been developed, based on the lubrication approximations, for predicting the time-evolution of the coating layer thickness of a complex liquid on a curved substrate. Substrate geometry is modeled as a time-independent overpressure distribution and the model includes such effects as evaporation, convection, and diffusion of solvent in the bulk liquid, and convection and diffusion of a soluble surfactant. For a given starting profile and substrate geometry, the temporal and spatial evolution of the free surface, bulk composition, surfactant concentration, surface tension, and layer-averaged viscosity are calculated until the drying process is complete. We show that convection of surfactant away from outside corners may slow the thinning in these regions. In addition, solvent evaporation may lead to Marangoni forces in the corner region, causing a ''rebound'' effect. Surface tension forces will initially displace liquid from corner regions, but the thinning will produce surface tension gradients which act to pull liquid back to the corner region. If the evaporation time scale is suitably matched to the time scale for flow induced by surface tension gradients, corner defects in the final dry coating layer can be substantially mitigated.

Key Words: **coating defects; surfactants; surface tension gradients; drying paint films; thin films; curved substrates.**

1. INTRODUCTION

Many industrial or natural processes involve the flow of thin liquid films. The most immediate application is the coating behavior of liquid paints. A freshly applied liquid film normally has an uneven surface. When surface tension can be considered to be uniform, capillary forces tend to reduce surface irregularities to produce a level film. This is the dominant effect leading to relatively uniform, or level, paint films, and for typical coating thicknesses is much more important than gravity, for example. A linear theory involving the use of the lubrication approximation, due to Orchard (1), predicts the rate of capillary-induced leveling and has met with considerable practical success.

The beneficial effect of surface tension, leading to more uniform coating layers, is limited largely to solid surfaces or substrates whose curvature variation is small. Indeed, in regions where the substrate is highly curved, surface tension can result in defects in the final coating: the coating tends to be thin at outside corners and to be thick or ''puddled'' at inside corners. Moreover, characteristic undulations can be found in the final coating near these corners. Typical corner defects, sometimes known as ''fat edges'' and ''picture-framing'' are illustrated schematically in Kornum and Raashou Nielsen (2) and are discussed further by Babel (3). While the fundamental process leading to corner defects can be demonstrated for a nonevaporating Newtonian liquid, an industrially useful mathematical model must incorporate compositional changes during drying. Since the surface tension of many complex liquids depends on bulk composition, spatial variation in composition for such liquids can lead to surface-tension-gradient or Marangoni effects. The resulting additional force on the liquid coating can modify the leveling history and the final film thickness distribution. For a flat substrate, this effect has been demonstrated by Overdiep (4) and Schwartz and Eley (5). In addition, Marangoni forces may arise due to surfactant or temperature gradients along the surface of the liquid film, as considered by Davis (6) and Jensen and Grotberg (7).

In previous work, for a nonevaporating Newtonian coating of constant viscosity, Schwartz and Weidner (8) showed that the effects of substrate curvature could be modeled by imposing an equivalent overpressure distribution on a nominally flat substrate. Overpressure variation causes the coating

[1] To whom correspondence should be addressed.

0021-9797/96 $18.00

to flow. Using the lubrication approximation, they calculated the evolving free-surface profiles on substrates of varying curvature for a liquid with constant surface tension. In this work, we extend the model to include the effects of surface tension gradients arising from two causes: (i) compositional changes in a two-component liquid model, and (ii) the presence of surfactants which may be distributed nonuniformly on the free surface of the coating. It will be shown that the development of surface tension gradients can dramatically alter the flow history of the coating layer.

A potential application of this work is improved protective coating of objects with corners of small radius. We illustrate the possibility of using surface-tension-gradient effects to counteract the tendency to form defects near corners. As the coating thins near an outside corner, for example, gradient forces can arise that will tend to draw liquid back to the thin region. We demonstrate that if the physical parameters describing the liquid coating are ''compatible'' with the rate of drying, the final dry film can be made significantly more uniform.

In the following section the thin-layer or lubrication evolution equation for a Newtonian liquid is reviewed and modified due to substrate curvature effects. Two-dimensional geometry is assumed. We model the coating as a two-component liquid composed of ''resin'' and ''solvent.'' Only the solvent evaporates, and, as it does, the resin fraction of the bulk liquid increases. The viscosity of the bulk liquid is a given function of resin concentration, becoming effectively infinite as the concentration tends to unity. The surface tension is assumed to vary with both bulk liquid concentration and surface concentration of a surfactant, which may or may not be soluble in the bulk liquid. The distribution of surfactant is modeled using a convection–diffusion equation which also includes transfer to and from the bulk liquid. Thus, in the model considered here, both surface tension gradients and substrate geometry drive the flow.

In section 3, the equations are reduced to nondimensional form. In terms of the dimensionless variables, it is shown that a wide class of substrate shapes produce equivalent flow behavior. The resulting similarity rules are valid for thin coating layers on substrates whose curvature is piecewise constant. Numerical results are presented in section 4. For definiteness we consider the evolution of an initially uniform coating layer on an outside corner. Simulated flow behavior, with and without surface-tension-gradient effects, are compared. When surface tension gradients arise solely from the forced motion of surfactant, corner defect formation can be partially inhibited. When the gradient-driven motion is caused by bulk compositional changes, on the other hand, it is demonstrated that a much greater degree of control of corner thickness is possible.

Additional conclusions arising from this study, and their implications for practical corner coating strategies, are presented in section 5.

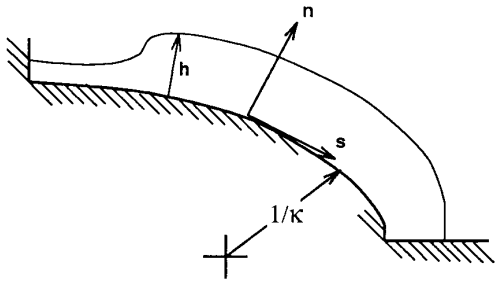

FIG. 1. Nomenclature and coordinate system.

2. MATHEMATICAL MODEL

The flow of Newtonian liquids is governed by the vector Navier–Stokes equation. With the ''lubrication'' assumptions, i.e., that the fluid layer is thin, the motion is slow, and the free surface is almost parallel to the substrate, the governing equation may be approximated as

$$p_s = \tau_n = \mu u_{nn}. \qquad [1]$$

Here subscripts signify partial differentiation, μ is viscosity, p is pressure, and u is the fluid particle velocity which is essentially parallel to the substrate. s and n are coordinates measured parallel and normal to the substrate, respectively. (See Fig. 1). The asymptotic validity of Eq. [1] has been well established (see, e.g., 9). The stress at the free surface τ_0 is equal to the surface tension gradient there (see 10),

$$\tau_0 = \sigma_s. \qquad [2]$$

Because of the thinness of the liquid layer, $p = p(s, t)$ only, and, assuming μ is also independent of n, [1] can be integrated immediately to give a parabolic velocity profile in n as

$$u(s, n, t) = \frac{\sigma_s}{\mu} n + \frac{p_s}{2\mu}(n^2 - 2hn), \qquad [3]$$

where $h = h(s, t)$ is the thickness of the coating layer. The total flux at any station s is given by

$$Q = \int_0^h u \, dn = \frac{h^2\sigma_s}{2\mu} - \frac{p_s h^3}{3\mu}, \qquad [4]$$

and integral mass conservation requires that

$$h_t = -Q_s - E = \left[-\frac{h^2\sigma_s}{2\mu} + \frac{h^3 p_s}{3\mu} \right]_s - E(s, t). \qquad [5]$$

Here $E(s, t)$ is the evaporation rate, with units of velocity, which may be a function of position and time.

Since the pressure outside the coating layer is assumed constant, the pressure gradient within the coating is due to variation in the product of surface tension and curvature at the liquid–vapor interface. The interface curvature may be considered to arise from the combined effect of substrate curvature and surface curvature relative to the substrate. Schwartz and Weidner (8) have shown that, subject to certain restrictions, the two contributions are approximately additive. Specific requirements are that the slope of the film relative to the substrate be small, as has already been assumed,

$$h_s \ll 1,$$

and, that the liquid film be thin,

$$h/R \ll 1. \qquad [6]$$

Here R is the local radius of curvature of the substrate. Then, within an error that is second-order small in h_s and first-order small in h/R, the pressure in the liquid can be approximated as

$$p = -\sigma\kappa - \sigma h_{ss}. \qquad [7]$$

A detailed derivation of Eq. [7] is given in Ref. 8. The net effect of this decomposition is to ''unwrap'' the curved substrate in the physical domain onto a straight surface, where the effect of substrate curvature is replaced by a time-independent distributed overpressure in the new computational domain. Here $\kappa = -1/R$ for a convex substrate. Substituting Eq. [7] in Eq. [5] yields

$$h_t = -\left[\frac{h^2\sigma_s}{2\mu} + \frac{h^3}{3\mu}\left(\sigma_s(\kappa + h_{ss}) + \sigma(\kappa_s + h_{sss})\right)\right]_s - E(s, t). \qquad [8]$$

For simplicity, the liquid is taken to consist of two components termed ''resin'' and ''solvent''; only the solvent component is assumed to be volatile. The resin fraction, or concentration c, is assumed to be uniform across the thin film. The validity of this ''well-mixed'' assumption requires certain restrictions on species diffusion, evaporation rate, and pressure gradients. If $T_{\text{dry}} \sim h/E$ is a characteristic time for drying and $T_{\text{diff}} \sim h^2/D^{(\text{r})}$ is the characteristic diffusion time, where $D^{(\text{r})}$ is the diffusion coefficient for resin in the bulk liquid, uniformity of c across the layer requires that

$$T_{\text{diff}} \ll T_{\text{dry}}$$

or

$$h \ll D^{(\text{r})}/E. \qquad [9]$$

Similarly, variation of c across the layer can result from forced convection along the layer produced by either pressure or surfactant gradients. This is because the velocity profile is nonuniform. The time scale for the development of significant values of $\partial c/\partial n$ from this source is

$$T_c \sim \frac{Lh}{Q}.$$

For $T_{\text{diff}} \ll T_c$, the concentration will be essentially uniform across the layer, which requires that

$$h \ll \frac{LD^{(\text{r})}}{Q}. \qquad [10]$$

Both criteria [9] and [10] are satisfied for sufficiently thin layers. Moriarty *et al.* (11) study the validity of the well-mixed model in more detail.

The resin fraction satisfies its own evolution equation which is taken to be

$$(ch)_t = -Q_s^{(\text{r})} = -(cQ)_s + (D^{(\text{r})}hc_s)_s. \qquad [11]$$

Observe that the resin flux $Q^{(\text{r})}$ is taken as the sum of two parts: (i) a proportionate share of the total flux Q, consistent with the well-mixed assumption, and (ii) a Fickian diffusion term driven by concentration gradients. It is reasonable to assume that the diffusivity $D^{(\text{r})}$ will decrease rapidly as the resin fraction, and consequently the viscosity increases; a simple assumption is that the diffusivity is inversely proportional to the viscosity. Such a relationship is known to be valid for dilute mixtures, as discussed by Probstein (12). Combining Eqs. [5] and [11] yields a convection–diffusion equation for concentration of the form

$$c_t = \left(\frac{E}{h}\right)c - \left(\frac{Q}{h}\right)c_s + \left(\frac{1}{h}\right)(D^{(\text{r})}hc_s)_s. \qquad [12]$$

The evaporation rate is assumed to vary as a power of the local solvent concentration

$$E(s, t) = E_0(1 - c)^{\alpha}, \qquad [13]$$

where exponent α may be determined from experimental or other data and is expected to lie in the range $(0 \leqslant \alpha < 1)$. E_0 is a constant with units of velocity. When $\alpha = 0$, the rate-controlling mechanism for evaporation is change of phase at the interface, resulting in a constant evaporation rate. For other α, the evaporation rate is a function of the availability of solvent molecules at the free surface.

It will prove useful to define the ''dry time'' as the time required for total solvent evaporation if the coating layer

were assumed to remain uniform in space. In this case, since the resin is conserved, h may be eliminated in favor of c using

$$ch = c_0 h_0, \qquad [14]$$

where c_0 is the initial concentration and h_0 is the initial film thickness. Integrating Eq. [5] readily yields

$$t_{\text{dry}} = \frac{c_0 h_0}{E_0} \int_{c_0}^{1} \frac{1}{c^2(1-c)^{\alpha}}\, dc. \qquad [15]$$

The integral can be expressed as a closed-form function of c_0 for certain values of α including the values 0 and $\frac{1}{2}$ as used below. For all cases of interest, where coatings dry nonuniformly in space, the time required for total drying everywhere will always exceed t_{dry}; yet t_{dry} serves as a useful *a priori* estimate for the total drying time.

The viscosity is taken to depend exponentially on the concentration, which is a simplified form of the law given by Patton (13) as

$$\mu = \mu_0 \exp[A(c - c_0)], \qquad [16]$$

where A is an empirically derived constant and μ_0 is the initial viscosity.

Local values of surface tension are assumed to depend on the concentration of surfactant on the free surface $c^{(s)}$ as well as on the local bulk composition c. In the first case, the surface concentration is determined by solving a convection–diffusion equation of the form

$$(c^{(s)})_t + (u^{(s)} c^{(s)})_s = D^{(s)}(c^{(s)})_{ss} + D^{(b)}(c^{(b)} - c^{(s)}). \qquad [17]$$

Here $u^{(s)}$ is the surface velocity which, from Eq. [3], will depend on local values of the bulk viscosity, pressure gradient, and surface tension gradient

$$u^{(s)} = u\,(n = h) = \frac{\sigma_s h}{\mu} - \frac{p_s h^2}{2\mu}. \qquad [18]$$

The nonlinear term on the left of Eq. [17] represents the combined effect of surfactant convection and concentration changes due to surface dilatation. $D^{(s)}$ is the surface diffusion constant for the surfactant. The last term on the right is a simple model for exchange of a soluble surfactant between the surface and bulk liquid. $c^{(b)}$ may be taken as a constant reference value; thus if, for example, the local value of $c^{(s)}$ is less than $c^{(b)}$, surfactant will be transferred to the surface at a rate determined by the constant $D^{(b)}$. Both terms on the right of Eq. [17] will tend to smooth out developed surfactant concentration gradients.

The surface tension is assumed to depend on the resin and surfactant concentrations via linear laws. Moreover the two effects are considered to be additive. If $\sigma^{(r)}$ is the surface tension of pure resin and $\sigma^{(s)}$ the surface tension of pure solvent, then the total surface tension can be written as

$$\sigma = \sigma^{(s)} + (\sigma^{(r)} - \sigma^{(s)})c + \Gamma(c^{(s)} - c_0^{(s)}), \qquad [19]$$

where $c_0^{(s)}$ is the initial concentration of surfactant, and Γ will be negative for surface active substances which lower the surface tension. Without loss of generality, the surfactant concentration $c^{(s)}$ can be considered nondimensional and, for an initially homogeneous coating, its initial value can be taken equal to one. The two reference constants, $c_0^{(s)}$ in Eq. [19] and $c^{(b)}$ in Eq. [17] can also be normalized to one. The intensity of surfactant effects will then be entirely incorporated in the remaining constants $D^{(s)}$, $D^{(b)}$, and Γ whose numerical values, for actual systems, can be determined from Langmuir trough or similar experiments (14).

3. NONDIMENSIONALIZATION AND SIMILARITY

Calculations shown below will consider the time evolution of a liquid coating layer of constant initial thickness h_0. This quantity is used as the reference length for dimensions normal to the substrate, while quantities involving distances along the surface will use a reference length L. The full nondimensionalization is

$$\begin{aligned} h &= h_0 \hat{h} \\ s &= L\hat{s} \\ \kappa &= \hat{\kappa}/L \\ \sigma &= \sigma_0 \hat{\sigma} \\ \mu &= \mu_0 \hat{\mu} \\ E &= \hat{E} h_0 / T^* \\ t &= T^* \hat{t} \end{aligned}$$

where

$$T^* = \frac{3\mu_0 L^4}{\sigma_0 h_0^3}$$

and σ_0 and μ_0 are the $t = 0$ reference values for surface tension and viscosity, respectively. T^* is the time scale for leveling first identified by Orchard (1).

In terms of the new dimensionless variables Eq. [8] is rewritten as

$$\hat{h}_{\hat{t}} = -\left[\frac{\hat{\sigma}_{\hat{s}}}{\hat{\mu}}\left(\frac{3}{2}\frac{L^2}{h_0^2}\hat{h}^2 + \frac{L}{h_0}\hat{h}^3\hat{\kappa} + \hat{h}^3\hat{h}_{\hat{s}\hat{s}}\right) + \frac{\hat{h}^3}{\hat{\mu}}\hat{\sigma}\left(\hat{h}_{\hat{s}\hat{s}\hat{s}} + \frac{L}{h_0}\hat{\kappa}_{\hat{s}}\right)\right]_{\hat{s}} - \hat{E}. \quad [20]$$

The first term multiplying $\hat{\sigma}_{\hat{s}}$ in Eq. [20] is greater than the second by a factor L/h_0 and is greater than the third term by a factor of L^2/h_0^2. Limiting our consideration to substrates with

$$\frac{h_0}{L} \ll 1$$

we shall neglect both smaller terms. (This is equivalent to the approximation employed in Eq. [6] with $R \sim L$.) Equation [20] reduces to

$$\hat{h}_{\hat{t}} = -\left[\frac{3}{2}\frac{L^2}{h_0^2}\frac{\hat{h}^2}{\hat{\mu}}\hat{\sigma}_{\hat{s}} + \frac{\hat{h}^3}{\hat{\mu}}\hat{\sigma}\left(\hat{h}_{\hat{s}\hat{s}\hat{s}} + \frac{L}{h_0}\hat{\kappa}_{\hat{s}}\right)\right]_{\hat{s}} - \hat{E}. \quad [21]$$

Using similar scaling arguments, the nondimensional form of the free surface velocity [18] takes the form

$$\hat{u}^{(s)} = \frac{3L^2\hat{\sigma}_{\hat{s}}\hat{h}}{h_0^2\hat{\mu}} + \frac{3\hat{\sigma}\hat{h}^2}{2\hat{\mu}}\left(\hat{h}_{\hat{s}\hat{s}\hat{s}} + \frac{L}{h_0}\hat{\kappa}_{\hat{s}}\right). \quad [22]$$

The dimensionless forms of the equations for the resin fraction and surfactant concentration, Eqs. [12] and [17], respectively, are identical to their dimensional forms, except for the introduction of the ''hatted'' quantities

$$\hat{Q} = \frac{QT^*}{h_0 L}$$

$$\hat{D}^{(s)} = \frac{D^{(s)}T^*}{L^2}$$

and

$$\hat{D}^{(b)} = D^{(b)}T^*.$$

As indicated in the previous section, the bulk diffusivity of resin is taken to be inversely proportional to the viscosity; therefore, equivalent to Eq. [16], we use

$$\hat{D}^{(r)} = \frac{K_D^{(r)}T^*}{L^2}\exp[-A(c - c_0)] = \hat{K}_D^{(r)}\exp[-A(c - c_0)], \quad [23]$$

where $K_D^{(r)}$ is the resin diffusion constant at $c = c_0$.

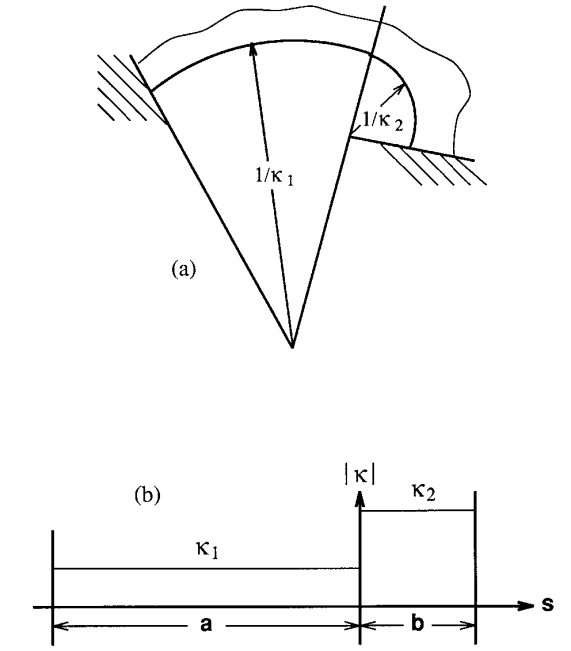

FIG. 2. (a) A substrate composed of two circular arcs with a continuous tangent. (b) The corresponding curvature distribution.

For definiteness, we will consider substrates with continuous tangent whose curvature is piecewise constant. In fact engineering representations of ''smooth'' boundary curves often consist merely of straight lines and circular arcs, with a continuous tangent where these ''pieces'' meet. A portion of a substrate consisting of two circular arcs of lengths a and b is shown in Fig. 2. At the ends of the domain shown, the coating surface is required to be parallel to the substrate and the fluxes Q are set equal to zero there. If the arc lengths and curvatures are suitably selected, various closed curves can be constructed by repeating and reflecting the portion shown. Such closed curves may be the cross sections of three-dimensional cylinders upon which coating is to be applied. The length of one of the arcs, a say, may be identified with the reference length L used above. Since fluid flow is driven only by curvature changes, this driving force is concentrated at the point where the two arcs meet. At this point $\hat{\kappa}_{\hat{s}}$ is singular.

While the phenomena of corner defects and their possible remediation using surface tension gradients is quite general, restricting consideration to the above class of shapes yields a significant simplification in the description of substrate geometry and makes it possible to concentrate more fully on flow behavior. In order to further reduce the complete specification of the general problem, only initially uniform coatings will be considered. The evolution equation then becomes

$$\hat{h}_{\hat{t}} = -\left[\frac{3}{2}\frac{a^2}{h_0^2}\frac{\hat{h}^2\hat{\sigma}_{\hat{s}}}{\hat{\mu}} + \frac{\hat{h}^3\hat{\sigma}}{\hat{\mu}}(\hat{h}_{\hat{s}\hat{s}\hat{s}} - M\delta(\hat{s}))\right]_{\hat{s}}, \quad [24]$$

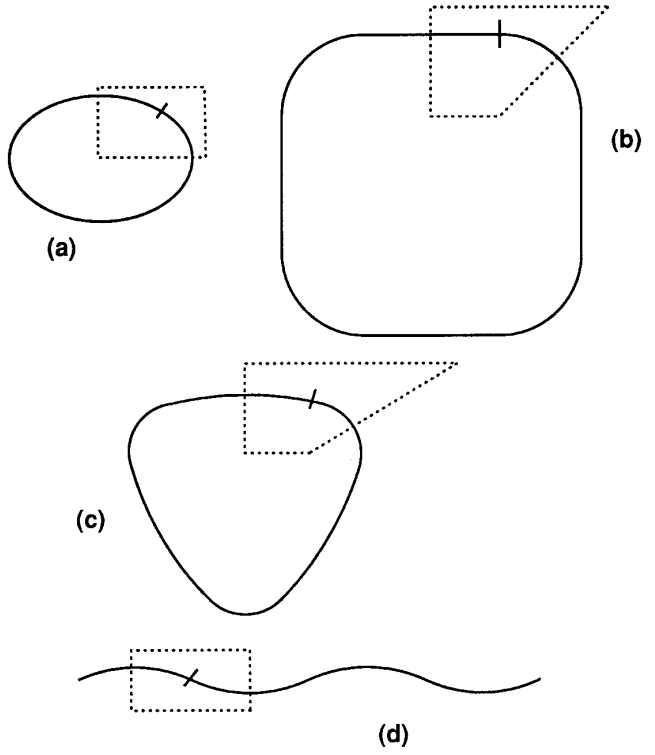

FIG. 3. Similar bodies for coating flow behavior, $a = b$, $a(\kappa_2 - \kappa_1) = \pi/4$. The location of the curvature discontinuity and the unit cell are shown for each body. The coating may be either outside or inside. Parameter values are (a) $a\kappa_1 = \pi/8$, $a\kappa_2 = 3\pi/8$; (b) $a\kappa_1 = 0$, $a\kappa_2 = \pi/4$; (c) $a\kappa_1 = \pi/24$, $a\kappa_2 = 7\pi/24$; (d) $a\kappa_2 = -a\kappa_1 = \pi/8$.

where $\delta(\hat{s})$ is the Dirac delta function. With $h(s, 0) = h_0$ and reflection boundary conditions imposed at the ends of the unit cell in Fig. 2, complete geometric specification is achieved by prescribing input values of a/b and

$$M = \frac{a^2(\kappa_1 - \kappa_2)}{h_0}.$$

A wide class of substrate or body shapes is equivalent in terms of coating flow behavior. Several equivalent body shapes are shown in Fig. 3 for the parameter values $a/b = 1$ and $a(\kappa_2 - \kappa_1) = \pi/4$. For cases a–c in Fig. 3, curvatures are selected so as to produce closed bodies, while case d is a periodically undulating substrate. Since flow is driven by curvature changes, results are independent of the absolute magnitude of substrate curvature. Thus for the shapes shown in the figure, equivalent problems arise independent of whether the coating is applied on the inside or outside of each shape.

The complete specification of the class of problems considered here requires a total of 12 dimensionless input parameters. Substrate geometry and initial layer thickness are given by

$$a/b,\ M,\ h_0/a.$$

The two-phase nature of the coating liquid, including the initial resin fraction, laws governing evaporation, viscosity, binary diffusivity, and surface tension variation, require an additional six parameters:

$$c_0,\ \hat{E}_0,\ \alpha,\ A,\ \hat{K}_D^{(r)},\ \Delta\sigma/\sigma_0,$$

where $\Delta\sigma = \sigma^{(r)} - \sigma^{(s)}$. Finally the presence of soluble surface-active material is allowed for by using three additional parameters:

$$\hat{D}^{(s)},\ \hat{D}^{(b)},\ \Gamma/\sigma_0.$$

While 12 dimensionless parameters is a formidable number, it is far fewer than would have arisen had the dimensional transformations, geometric similarity and various simplified formulas not been used. By keeping the full problem relatively simple, it is possible to give some indication of the expected flow histories under the combined influence of several effects. It is anticipated that more accurate laws, to the extent that they are known for particular systems, could be inserted in the numerical simulations without additional difficulty. For ease of interpretation, the numerical results reported below are given in physical units for a nominal right-angle outside corner. They are, in fact, equally applicable to other shapes, as has been indicated above. Thus ''puddling'' at inside corners is caused by essentially the same effect as outside-corner thinning, and remediation by use of developed surface tension gradients is equally valid for those cases.

4. NUMERICAL IMPLEMENTATION AND RESULTS

The evolution Eq. [21] together with Eq. [17] are discretized and solved numerically using central finite differences. The numerical treatment of the delta function in Eq. [24] is examined in Schwartz and Weidner (8), and also in Weidner (15). Time integration is done semi-implicitly in the sense that the nonlinear prefactors $\hat{h}^2$ and $\hat{h}^3$ in Eq. [20] are evaluated at the old time level. For a fully explicit scheme, where all terms are evaluated at the old time level, permissible time steps must be very small for numerical stability. Use of the present implicit scheme allows a speed up of several orders of magnitude. Details of the numerical implementation can be found in Moriarty *et al.* (16) and Schwartz and Eley (5).

In this section we use our numerical simulation to explore the effects of surface-tension gradients on the coating behavior of a model coating on a curved substrate. Specifically we consider an initially uniform coating on an outside corner

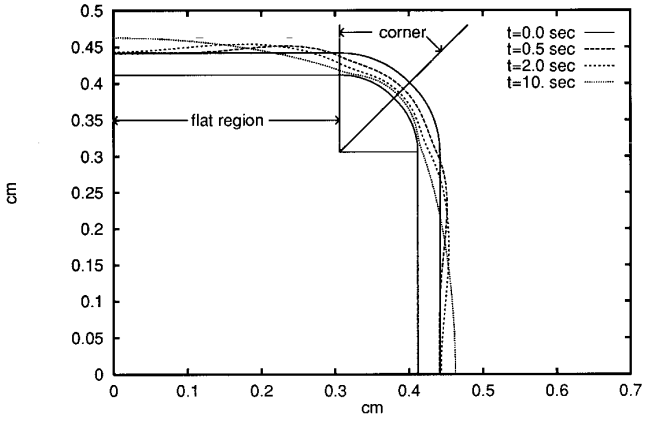

FIG. 4. Reference case for flow away from an outside corner for a nonevaporating Newtonian liquid of constant surface tension. Here the corner radius is 0.1 cm. The coating profiles are shown at various times. Note that the thickness of the coating layer has been magnified by a factor of 3 for clarity. Dimensionless parameters for this case are $a/b = 4$, $M = 100$, and $h_0/a = 0.0318$.

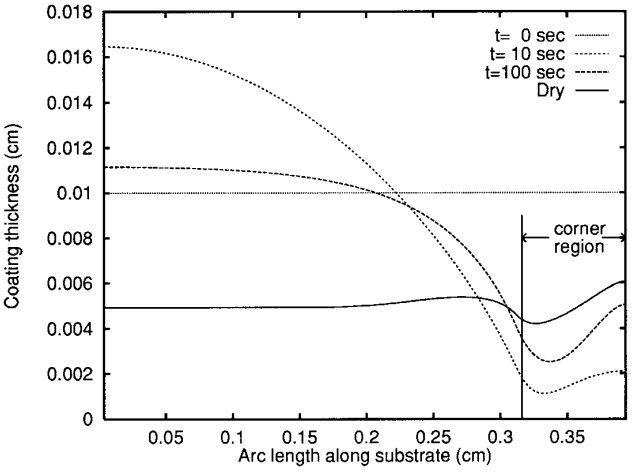

FIG. 6. Sequence of coating profiles for model coating with $\alpha = 0.5$, and $E_0 = 1.36 \times 10^{-5}$ cm/s, corresponding to a dry time of 14.0 min. Here $\Gamma = 0.0$ dyn/cm, $\Delta\sigma = 6.0$ dyn/cm, $A = 15.0$, and $K_D^{(r)} = 2 \times 10^{-5}$ cm^2/s. Dimensionless parameters for this case are $\hat{E}_0 = 1.44$, $\hat{K}_D^{(r)} = 0.215$, and $\Delta\sigma/\sigma_0 = 0.218$.

with a radius of 0.1 cm with $a/b = 4$. (See Fig. 4.) For convenience, the results are presented in physical units. For our model coating the initial surface tension is 27.5 dyn/cm and the initial viscosity is 1.0 poise. The initial concentration is 0.5 and the initial coating layer is uniform with a thickness $h_0 = 0.01$ cm. Other parameters vary and their values will be included in the figure captions.

Figure 5 shows the evolving coating profile for an outside corner. For clarity we have chosen to plot coating thickness versus arc length along the substrate; i.e., the body surface has been ''unwrapped.'' For reference, Fig. 4 shows the same profiles in the original or ''physical'' plane. In this simulation there is no evaporation or surface tension gradients. Note how quickly the coating thins in the corner region: in 10 s the coating thickness has been reduced to less than 20% of its initial value.

We first investigate the effects of surface tension gradients

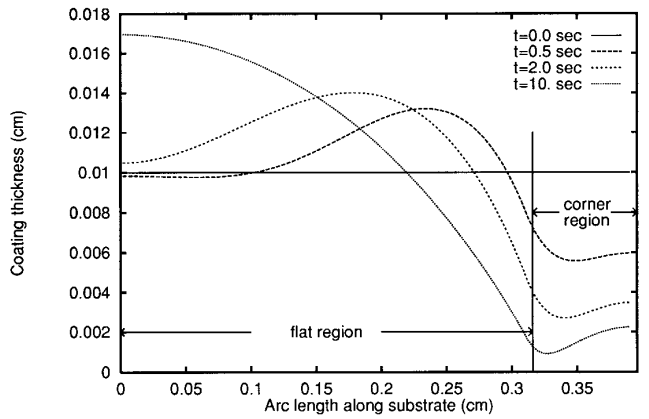

FIG. 5. Coating height variation versus arc length for the same case as described in the legend to Fig. 4.

due to compositional changes in the liquid. Combining Eqs. [14] and [13] we find that evaporation causes the concentration to increase at a rate inversely proportional to h: $c_t \sim 1/h$. Consequently the resin concentration will increase at a faster rate in regions where the coating layer is thin compared to regions with a thick coating layer. Typically the surface tension of the resin is greater than that of the solvent, and in this case the evaporation induced concentration gradients will lead to surface tension gradients which act to pull the coating from thick regions toward thin regions. For sufficiently strong surface tension gradients, the surface traction generated can counteract the thinning effects caused by substrate curvature.

Figure 6 shows the evolving profiles of our model coating at four different times. Here the evaporation rate is $E_0 = 1.36 \times 10^{-5}$ cm/s, and $\alpha = 0.5$, corresponding to a dry time of 14.0 min. The surface tension of the resin is higher than that of the solvent by 6.0 dyn/cm ($\Delta\sigma = 6$), $K_D^{(r)} = 2 \times 10^{-5}$ cm^2/sec, and $A = 15.0$. At $t = 10$ s, very little of the solvent has evaporated and most of the coating has been displaced from the corner region, exactly as in the nonevaporating case shown in Fig. 5. But in contrast to the nonevaporating case, where h in the corner region continues to monotonically decrease, here the thickness of the coating layer in the corner region first decreases to a minimum value and then begins to increase. At $t = 10$ s, the minimum value of h in the corner region is approximately one-tenth the maximum h in the flat region. According to the mechanism described above, we expect evaporation to lead to strong surface tension gradients in this region, which will act to pull liquid from the flat region toward the corner. The result of this process is to cause a ''rebound'' effect. This is illustrated by the $t = 100$ s profile in Fig. 6, where the volume of liquid

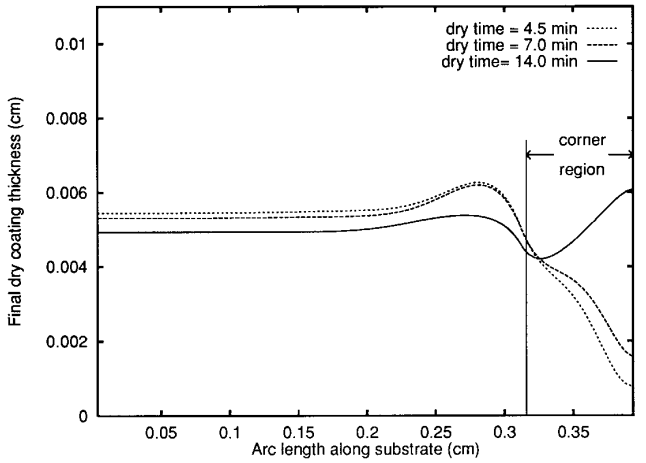

FIG. 7. Final dry coating profiles for various dry times. Here $\alpha = 0.5$, corresponding to a dry time of $t_{\text{dry}} = 1.14\, h_0/E_0$, $\Gamma = 0.0$ dyn/cm, $\Delta\sigma = 6.0$ dyn/cm, $A = 15.0$, and $K_D^{(r)} = 2 \times 10^{-5}$ cm^2/s. Dimensionless parameters for this case are $\hat{E}_0 = 4.48$, $\hat{E}_0 = 2.88$, $\hat{E}_0 = 1.44$ for the 4.5-, 7.0-, and 14.0-min dry time cases, respectively; $\hat{K}_D^{(r)} = 0.215$; and $\Delta\sigma/\sigma_0 = 0.218$.

in the corner region is approximately twice the volume at $t = 10$ s.

Once surface-tension gradients have reached a level sufficient to reverse the net flux away from the corner, the magnitude of the surface tension gradients begins to decrease due to convection of solvent-rich liquid from the flat region into the corner region, as well as the continuing effects of resin diffusion in the bulk liquid and the increase in the coating thickness in the corner region. (The increase in coating thickness in the corner region slows the effect which initiated the rebound: for the $t = 100$ s profile in Fig. 6, the minimum coating thickness is only one-fourth the maximum value.) For the case illustrated by Fig. 6, the surface tension gradients remain strong enough to continue to counter the effects of the overpressure, resulting in a final dry coating thickness at the corner which is actually greater than the average dry coating thickness of 0.005 cm.

The increase in resin concentration during the initial thinning phase in the corner region causes an exponential increase in viscosity in this region (following Eq. [16]). Hence the magnitude of the surface tension gradients must be strong enough to overcome not only the effects of the overpressure in the corner, but also a larger viscosity here, which lowers any net flux. Figure 7 shows the final dry coating profiles of our model coating for three different values of t_{dry} (corresponding to three different values of E_0). For the 4.5-min dry time case, the increase in viscosity in the corner region has prohibited a full rebound effect, and the final dry coating thickness at the corner is less than 20% of the average dry coating thickness. For the 7.0-min dry time case, the increase in viscosity has been slow enough to allow for a partial rebound effect, but the fast evaporating solvent has still ''frozen'' the coating thickness at the corner before convection of solvent-rich coating from the flat region has reached the corner. Only for the 14.0-min dry time case do we observe the full rebound effect. For this case, the time scales associated with the increase in viscosity in the corner region, and the development of surface tension gradients over the flat region, allow for convection of liquid all the way into the corner before the increase in viscosity due to evaporation limits this flux.

For a given viscosity–concentration relationship, the presence of this rebound effect depends on the drying time and the magnitude of $\Delta\sigma$. Figure 8 shows the dependence of the dry coating height at the corner versus the drying time for various values of $\Delta\sigma$. These results demonstrate that if the solvent evaporates too fast, corresponding to short dry times, then the corresponding rise in viscosity prohibits the rebound effect. Conversely, for low evaporation rates (long dry times), the viscosity increase will be slow and the time scales associated with the increase in viscosity in the corner region and the development of surface tension gradients may allow for a rebound effect for a large enough $\Delta\sigma$. The larger $\Delta\sigma$, the larger the traction drawing the coating back toward the corner region and the thicker the final dry coating thickness at the corner. As remarked above, the surface tension gradients which have caused the rebound effect begin to decrease immediately following the rebound. This accounts for the decline in the final coating thickness at the corner for the $\Delta\sigma = 6$ dyn/cm and $\Delta\sigma = 5$ dyn/cm cases at long dry times.

Figures 9 and 10 demonstrate the effect of surfactants on the thinning due to substrate curvature. For these two cases, the evaporation rate is $E_0 = 1.36 \times 10^{-5}$ cm/s, and $\alpha = 0.5$, corresponding to a dry time of 14.0 min. Here we assume that the resin has the same surface tension as that of the

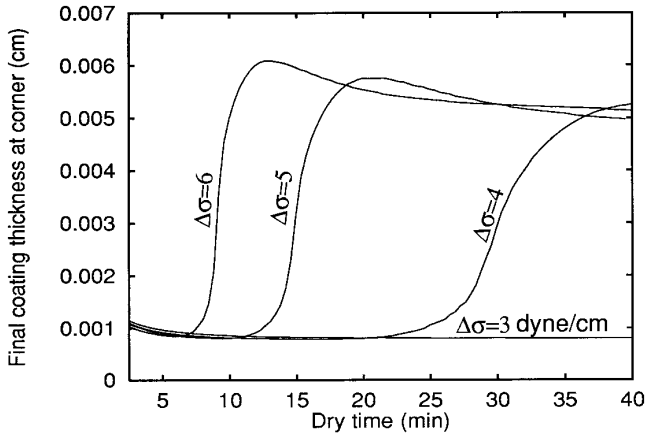

FIG. 8. Comparison of final dry corner thickness (h at $s = 3.93$ cm) for various values of $\Delta\sigma$. Here $\alpha = 0.5$, corresponding to a dry time of $t_{\text{dry}} = 1.14\, h_0/E_0$, $\Gamma = 0.0$ dyn/cm, $A = 15.0$, and $K_D^{(r)} = 2 \times 10^{-5}$ cm^2/s. Dimensionless parameters are $0.5 \leqslant \hat{E}_0 \leqslant 8.08$, $\hat{K}_D^{(r)} = 0.2153$, and $0.109 \leqslant \Delta\sigma/\sigma_0 \leqslant 0.218$.

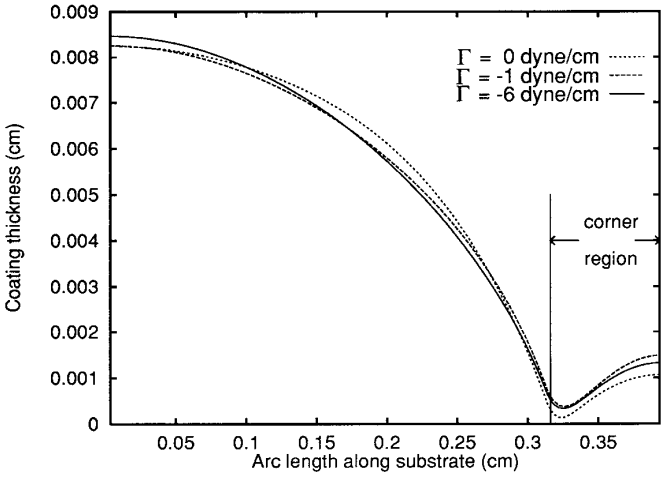

FIG. 9. Final dry coating profiles for various values of Γ. Here $\Delta\sigma = 0$, $D^{(s)} = 1.0 \times 10^{-5}$ cm^2/s, $D_b = 0.0$ s^{-1}, $\alpha = 0.5$, and $E_0 = 1.36 \times 10^{-5}$ cm/s, corresponding to a dry time of 14.0 min. Dimensionless parameters are $\hat{E}_0 = 1.45$, $\hat{D}^{(s)} = 0.108$, $\hat{D}_b = 0.0$, and $3.63 \times 10^{-3} \leqslant -\Gamma/\sigma_0 \leqslant 2.18 \times 10^{-2}$.

solvent: evaporation causes only an increase in the viscosity, not surface tension. The diffusion coefficient of surfactant on the free surface is taken as $D^{(s)} = 1.0 \times 10^{-5}$ cm^2/s which is a typical value from Ref. 17 and diffusion of surfactant to and from the bulk is ignored, corresponding to an insoluble surfactant.

In the process of thinning, the surface velocity is directed away from the corner region and surfactant is carried from the corner region to the flat region. Because surfactant acts to decrease the surface tension of the coating, the surface tension in the corner region will be greater than in the flat region. This surface tension gradient acts to pull liquid from the flat region to the corner region, potentially counteracting the effect of the overpressure distribution. Figure 9 shows the final dry coating profiles for two cases with surfactant: $\Gamma = -1$ dyn/cm corresponding to a ''weak'' surfactant, and $\Gamma = -6$ dyn/cm, corresponding to a ''strong'' surfactant, as well as a test case with no surfactant, given by $\Gamma = 0$. Though the two cases with surfactant have led to a thicker final coating in the corner region compared to the test case, the surface tension gradients developed as a result of the convection of surfactant are strong enough only to *slow* the thinning in the corner region, not reverse the effect. Moreover, a close inspection of Fig. 9 shows that the $\Gamma = -1$ dyn/cm case actually results in a thicker final coating in the corner region compared to the $\Gamma = -6$ dyn/cm case. This anomalous effect is best explained by examining Eq. [18]. For the case considered here, p_s, the pressure gradient caused by the overpressure and σ_s, the surface tension gradient caused by convection of surfactant, are both positive in the vicinity of the corner. In the initial stages of thinning, σ_s is small and both the surface velocity and the net flux are negative (away from the corner). As the thinning proceeds, surfactant gradients cause an increase in σ_s, lowering the magnitude of the surface velocity, and consequently slowing the convection of surfactant from the corner onto the flat region. When $\sigma_s > p_s h/2$ the surface velocity actually changes direction, and surfactant is carried back into the corner, causing a decrease in the magnitude of the surface tension gradient. Note that the net flux may remain negative even when the surface velocity is positive. (From Eq. [4], this condition can occur when $p_s h/2 < \sigma_s < 2p_s h/3$.) Because of this counterbalancing effect, increasing the strength of the surfactant may only decrease the thinning during the initial stages: The final dry coating profile depends on the resistance to the overpressure by surface tension gradients through the entire drying process.

Figure 10 illustrates this effect. Here we plot the coating thickness at the corner as a function of time for the same case as Fig. 9. Note the ''crossover'' of the curves for $\Gamma = -1$ and $\Gamma = -6$ dyn/cm at approximately 8 s. For times less than 8 s, the coating with $\Gamma = -6$ dyn/cm resists the thinning in the corner better than the $\Gamma = -1$ dyn/cm case, for in the early stages of thinning the stronger surfactant develops a stronger surface tension gradient from the initial convection-induced surfactant gradient. But due to this surface tension gradient, convection of surfactant away from the corner is retarded, and eventually reversed, causing a decrease in the surfactant gradient, and consequently a decrease in the magnitude of the surface tension gradient which is helping to oppose the flux away from the corner. In contrast, the weaker surfactant is unable to develop sufficiently strong surface tension gradients in the early stages of the thinning, but during this period the surface velocity continues to cause convection of surfactant away from the corner.

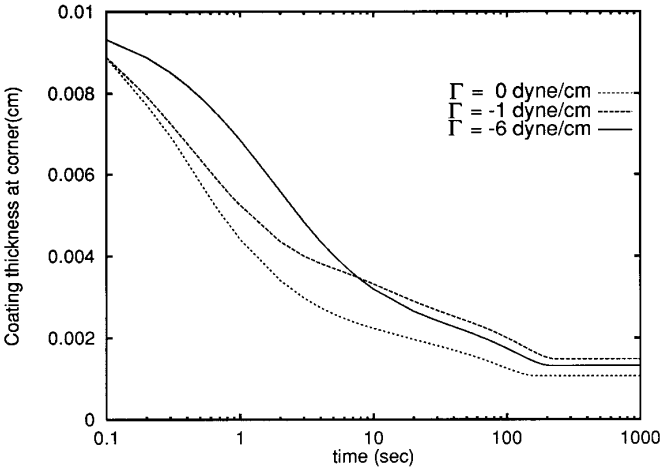

FIG. 10. Time evolution of coating thickness at corner (h at $s = 3.93$ cm) for various values of Γ. Here $\Delta\sigma = 0$, $D^{(s)} = 1.0 \times 10^{-5}$ cm^2/s, $D_b = 0.0$ s^{-1}, $\alpha = 0.5$, and $E_0 = 1.36 \times 10^{-5}$ cm/s, corresponding to a dry time of 14.0 min. The time axis employs a log scale for clarity. Dimensionless parameters are $\hat{E}_0 = 1.45$, $\hat{D}^{(s)} = 0.108$, $\hat{D}_b = 0.0$, and $3.63 \times 10^{-3} \leqslant -\Gamma/\sigma_0 \leqslant 2.18 \times 10^{-2}$.

As a result, the decrease and eventual reversal of the surface velocity does not occur until much later for this case. Consequently the surface tension gradients are effective in opposing the thinning effects of the overpressure, for a longer period of time compared to the $\Gamma = -6$ dyn/cm case. There appears to be a critical value for Γ which leads to the best protection in the corner region for this particular case, though even with an optimal Γ, the final dry coating is substantially thinner in the corner compared to the average dry coating.

5. CONCLUSIONS

Due to the large number of dimensionless parameters required to completely specify the physics of a drying film on an arbitrarily curved substrate, even with the many simplifications employed in our model, we have limited our scope to the canonical problem of an evaporating film in the vicinity of a an outside corner of small radius, and considered only a very narrow range of possible geometric parameters and physicochemical coating properties. Moreover, different viscosity–bulk concentration, surface tension–bulk concentration, surface tension–surfactant concentration, and other laws may more accurately model many coatings of industrial interest. Nonetheless, we believe that the qualitative results of our investigation are sufficiently robust to remain valid for a large range of practical coating problems. We have shown that surface tension gradients play a strong role in the dynamics of a drying film in the vicinity of sharp corners, and may even help remediate coating defects common to these applications.

The simulations indicate that the presence of surface tension gradients due to convection of surfactants slow the thinning due to substrate geometry, but that increasing the quantity or strength of surfactant will not necessarily lead to a thicker final coating. Surface tension gradients due to compositional changes in a multicomponent coating liquid resist thinning by a different mechanism. Here the coating in the corner region must be substantially reduced from the initial thickness before surface tension gradients become strong enough to cause the coating to be pulled back onto the corner region. As the solvent evaporates, the viscosity increases, particularly in the corner region where the coating is thin. Thus the surface tension gradients must be strong enough to overcome the increased viscosity of the rapidly drying coating as well as the tendency for the coating to thin in the corner due to substrate geometry. There appears to be a critical relation between the drying time and $\Delta\sigma$ required to produce a rebound effect. Without the rebound, the dry coating layer in the corner region may be too thin to adequately protect the substrate. These results are of particular relevance at this time due to the legislation mandated reductions in the allowed levels of volatile organic compounds in many industrial paint formulations. These new paints generally have quite different physicochemical properties than the coatings they replace and frequently exhibit poorer coating performance in many coating applications. Because many objects of practical and industrial interest have sharply rounded corners which require a protective or decorative coating, the role of surface tension gradients during the drying process should not be ignored. In fact, it may be possible to adjust the physical parameters of the coating formulation and the rate of drying to produce substantially more uniform coatings on sharp corners.

ACKNOWLEDGMENT

This work has been supported, in part, by the ICI Strategic Research Fund.

REFERENCES

1. Orchard, S. E., *Appl. Sci. Res. A* **11,** 451 (1962).
2. Kornum, L. O., and Raashou Nielsen, H. K., *Prog. Org. Coat.* **8,** 275 (1980).
3. Babel, E., *Plaste Kautsch.* **21,** 695 (1974).
4. Overdiep, W. S., *Prog. Org. Coat.* **14,** 159 (1986).
5. Schwartz, L. W., and Eley, R. R., *Prog. Org. Coat.,* in press.
6. Davis, S. H., *Annu. Rev. Fluid Mech.* **19,** 403 (1987).
7. Jensen, O. E., and Grotberg, J. B., *Phys. Fluids A* **5,** 58 (1993).
8. Schwartz, L. W., and Weidner, D. E., *J. Eng. Maths.* **29,** 91 (1995).
9. Sherman, F. S., ''Viscous Flow.'' McGraw–Hill, New York, 1990.
10. Landau, L., and Lifshitz, E., ''Fluid Mechanics.'' Pergamon, Oxford, 1959.
11. Moriarty, J. A., Terrill, J. A., and Wilson, S. K., *in* ''Proceedings of the 8th European Conference on Mathematics in Industry'' (H. Neunzert, Ed.). Teuber, Stuttgart, in press, 1996.
12. Probstein, R. F., ''Physicochemical Hydrodynamics,'' 2nd ed. Wiley, New York, 1994.
13. Patton, T. C., ''Paint Flow and Pigment Dispersion.'' Wiley, New York, 1979.
14. Eley, R. R., Zander, R. A., and Koehler, M. E., *in* ''Water-Soluble Polymers: Beauty with Performance'' (J. E. Glass, Ed.), p. 315. Am. Chem. Soc., New York, 1986.
15. D. E. Weidner., ''Numerical Simulation of Coating Flows.'' Ph.D. thesis, University of Delaware, 1993.
16. Moriarty, J. A., Schwartz, L. W., and Tuck, E. O., *Phys. Fluids A* **3,** 733 (1991).
17. Sakata, E. K., and Berg, J. C., *Ind. Eng. Chem. Fund.* **8**(3), 570 (1969).